

FAT: Training Neural Networks for Reliable Inference Under Hardware Faults

Ussama Zahid*, Giulio Gambardella*, Nicholas J. Fraser*, Michaela Blott*, Kees Vissers†

*Xilinx Research Labs, Dublin, Ireland, Email: {ussamaz, giuliog, nfraser, mblott}@xilinx.com

†Xilinx Research Labs, San Jose, USA, Email: keesv@xilinx.com

Abstract—Deep neural networks (DNNs) are state-of-the-art algorithms for multiple applications, spanning from image classification to speech recognition. While providing excellent accuracy, they often have enormous compute and memory requirements. As a result of this, quantized neural networks (QNNs) are increasingly being adopted and deployed especially on embedded devices, thanks to their high accuracy, but also since they have significantly lower compute and memory requirements compared to their floating point equivalents. QNN deployment is also being evaluated for safety-critical applications, such as automotive, avionics, medical or industrial. These systems require functional safety, guaranteeing failure-free behaviour even in the presence of hardware faults. In general fault tolerance can be achieved by adding redundancy to the system, which further exacerbates the overall computational demands and makes it difficult to meet the power and performance requirements. In order to decrease the hardware cost for achieving functional safety, it is vital to explore domain-specific solutions which can exploit the inherent features of DNNs. In this work we present a novel methodology called fault-aware training (FAT), which includes error modeling during neural network (NN) training, to make QNNs resilient to specific fault models on the device. Our experiments show that by injecting faults in the convolutional layers during training, highly accurate convolutional neural networks (CNNs) can be trained which exhibits much better error tolerance compared to the original. Furthermore, we show that redundant systems which are built from QNNs trained with FAT achieve higher worst-case accuracy at lower hardware cost. This has been validated for numerous classification tasks including CIFAR10, GTSRB, SVHN and ImageNet.

Index Terms—Neural Networks, Safety, Functional Safety, FPGA, Quantized Neural Networks, Dropout2D, Training

I. INTRODUCTION

CNNs have recently gained significantly in popularity due to their high accuracy in numerous applications such as image classification [1], object detection and localization [2], image segmentation [3, 4]. In some applications, such as image classification, CNNs can even outperform human beings [5]. Nonetheless, the push for accuracy increase came at the cost of escalating computational and memory demands. This in turn, started many branches of research targeting reducing the deployment cost of CNNs. These techniques include: direct quantization [6], quantization-aware training [7–10], pruning and compression [11], using less intensive layers (depth-wise separable convolutions [12]), non-arithmetic layers (e.g., ShiftNet [13]). Reduced precision DNNs reduce the memory footprint compared to a full precision one, sometimes incurring in modest drop in accuracy, which can be compensated with network topology changes [14]. Reduced precision DNNs

have weights and activations for which possible values are restricted within a few bits, thus requiring smaller adders and multipliers in hardware for the involved multiply-accumulate (MAC) operations as compared to floating point DNNs. This is especially true on reconfigurable hardware, on which it is possible to tailor hardware to the needed precision, enabling scaling of parallelism when hardware cost is decreased. Additionally, quantization makes it easier to deploy DNNs on small embedded devices for real-time applications [15]. FINN [16] is one of the frameworks which demonstrates an efficient way of deploying QNNs on field programmable gate arrays (FPGA) which leverages quantization to achieve high throughput in terms of frames per second (FPS).

In order to use an electronic device in a safety critical application, its dependability must be evaluated. This consists of four components: reliability, availability, maintainability and safety (RAMS) [17]. The safety analysis and its evaluation is regulated by the standards depending on the application domain (e.g., IEC-61508 for industrial systems, ISO-26262 for road vehicles and EN 50126/8/9 for rail transport), with safety levels proportional to the criticality of the specific task. Failure, modes, effects, and diagnostic analysis (FMEDA) [18] have to be evaluated for each of the components of the design in order to model the safety features of the system.

During deployment, when a DNN is running on some execution hardware, there is a non-zero probability of the hardware malfunctioning. This malfunctioning can be caused by permanent or transient hardware faults. Common sources of transient errors are direct or indirect ionization, mostly by means of heavy ions. This is especially true for avionics or space applications where protons are likely to hit hardware circuit and generate transient effects. Permanent faults are instead commonly linked with electrical failures in digital circuits, like electromigration, aging (due to hot-carrier injection (HCI) or negative bias temperature instability (NBTI)). Electrical faults will often cause a disconnection in wiring along with a misbehaviour in the functioning of a transistor, which can lead to open or short circuits in the output of a logic gate. Two common errors which can arise in the computation from hardware faults are single-event-effects (SEEs) (transient) and stuck-at (permanent). The result of SEEs is usually a single-bit error in a stream of data, or a bit-flip in a memory array. Stuck-at errors usually correspond to some larger fault within the hardware, which causes the output of a particular circuit to have a singular value. A stuck@x fault refers to this type

of fault, where a given value in a circuit is always stuck at the value x , rather than the value intended by the circuit itself. Note that on FPGAs, if no measures like scrubbing are adopted, permanent errors can occur from transient fault effecting the FPGA configuration memory. In order to safely adopt DNNs in safety critical applications, it is required that they must be tolerant to different fault models. QNNs tolerance measurements can be done through *error injection*, which can be used to evaluate the accuracy in the presence of possible errors, as presented by Gambardella et al. [19] and Khoshavi et al. [20]. In this work, we propose a novel training method which leverages error modelling during the training process of QNNs in order to make them resilient to particular errors when deployed for inference in the field. The main contributions of this paper are:

- an efficient methodology (FAT) to train error tolerant QNNs;
- an evaluation of our methodology compared to Dropout2D [21] as an alternative method to introduce fault tolerance in the QNNs; and
- a hardware cost vs. worst case error analysis of FAT trained QNNs vs. QNNs trained with standard quantized neural network training techniques, which we denote as standard training (SAT).

This paper is organised as follows: Section II describes different types of QNN accelerators and introduces some error models which can arise from faults in QNN hardware; Section III discusses prior work related to the fault tolerance of QNNs and introduces a motivating example for this work; Section IV introduces our proposed methodology; and finally Sections V to VII contain results, discussions and conclusions respectively.

II. BACKGROUND

CNNs are usually composed of a sequence of layers, each with its own characteristics such as: feature map sizes, channels and filters. We refer the readers to the works by Mittal [22] and Venieris et al. [23] for an exhaustive list of CNN accelerators targeting programmable logic. In this paper, we adopt the QNN accelerators code-named FINN [16, 24] which are publicly available on GitHub [25]. Blott et al. [24] presented two different hardware architectures, namely *dataflow* and *loopback*. In *dataflow*, all layers are concurrently offloaded in programmable logic, with each layer mapped to its own array of processing elements (PEs). Each array executes a single layer in a folded fashion, meaning each PE is computing 1 or more outputs (e.g., an entire channel of an output feature map (OFM)) of a *single* layer.

In *loopback*, a single array of PEs computes the CNN output, computing each layer in sequential manner. This implies that each PE is computing 1 or more output of *multiple* layers.

Independently from the hardware architecture, possible faults in any of the PEs can present themselves as errors in the intermediate values of the CNN during inference time. These errors are likely to have different properties based on

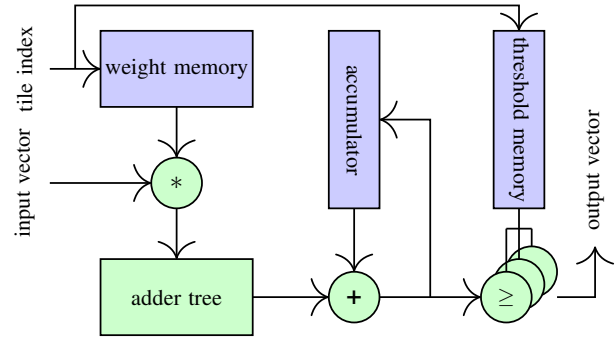


Fig. 1: Matrix Vector Threshold Unit (MVTU) block diagram, core component of a PE in FINN

the design of the CNN execution engine and the nature of the fault which occurs.

The portion of the network affected by a corrupted PE depends upon the scheduling of the CNN and the architecture of the hardware accelerator. For example in FINN *dataflow*, each PE is scheduled for computing one or more entire OFM channels of only one layer. If a PE of a specific layer is faulty, the OFM channels (of that particular layer) which are being calculated by the faulty PE, are potentially erroneous. Whereas in the *loopback* architecture, PEs are being used to execute multiple layers. Hence a fault in any of the PEs will effect one or more OFM channel(s) of *multiple* layers. Similarly, if with a different scheduling each PE is computing a particular pixel for all channels, faulty PE would result in same pixel being erroneous for all OFM channels. In general, depending on the hardware architecture and on the scheduling, different models should be used to better represent possible permanent errors of the CNN accelerator.

In the remainder of the paper we will focus on two main error models: single channel stuck@ errors and same pixel in all channels stuck@. The former cause an entire output channel of a particular layer being stuck-at, while the latter has all channels in the same pixel containing the same value.

With the FINN architecture, channel stuck@ models the possible faults within a single PE, composed of MAC and activation block (called matrix vector threshold unit (MVTU)) as shown in Figure 1. In the MVTU architecture, a faulty bit in the input vector, adder tree, weight memory or in the multiplier will most likely affect the accumulator value. Faults in the threshold memory or in the comparators would have effects on the result of the output vector. All of the above faults, if not masked, could thus result in an error in the output activation. In the worst case scenario, the error would be propagated to the entire output channel, given the adopted scheduling. On the other hand, pixels stuck@ in FINN models the faults in the communication between layers, since each layer produces streams of all channels for a single pixel, and pixels are generated in a raster order. A possible fault in the communication FIFO would then result in a complete pixel being compromised.

In this work, we focus on QNNs with different precisions for weights \mathbf{W} and activations \mathbf{A} , denoted as $\mathbf{W}_w\mathbf{A}_a$, where

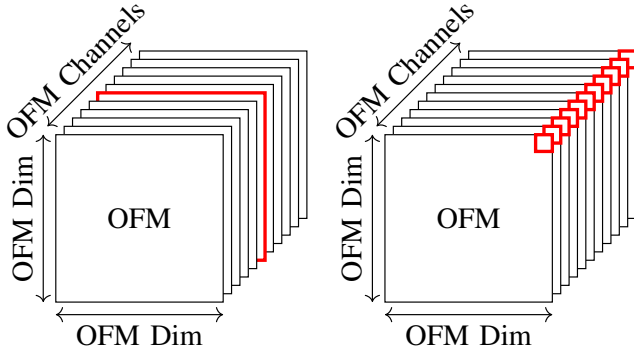


Fig. 2: Possible error models due to faulty PE, channel stuck@ (left) and same pixel stuck@ (right)

w is the weights bit width, and a is the activation bit widths. Different errors can appear in the output activation depending on the precision. For example in FINN for 1 bit activation, possible stuck@ values are $\{0$ (representing -1), $1\}$. For 2 bits activation, since we are using symmetric quantization, the possible stuck@ values are $\{-1, 0, 1\}$.

III. RELATED WORK

In the domain of self driving cars, recent works [26–28] have tried to assess the safety of DNNs. If we look at the prior work done in making DNNs error tolerant, most of the literature targets multi-layer perceptrons (MLPs), focusing mainly on stuck@0 faults [29–34]. They propose different training methodologies to make MLPs robust to errors. Deodhare et al. [29] formulated fault tolerance as a min-max optimization problem. They present two different methods to solve this min-max problem. The resulting NN from both method though not always fault tolerant, exhibits acceptable degree of partial fault tolerance to the loss of single node (neuron) and its associated weights (representing stuck@0 error). Dey et al. [30] includes the weighted sum of some special terms in the loss function (e.g. sum of squares of first/second derivatives of loss w.r.t weights and L2 norm of the weight vector) during training. They showed on 20 different datasets that resulting MLP is robust to link-failures (stuck@0) and uncertainty in weights caused by additive or multiplicative noise. Tan and Nanya [31] train with stuck@0 faults injected during training and enhance the generalization ability of the MLP. They study the relationship between fault tolerance and generalization and also show 6% improvement in accuracy when training with error injection. More recently, researchers have started looking into fault tolerance for CNNs, such as the work by Duddu et al. [34] implements adversarial training for the feature extractor of CNN and uses supervised training for the classifier to make it robust to stuck@0 errors only. We are not aware of any works which attempt to train QNNs to be robust to stuck@ errors, nor are we aware of any works which train CNNs to be robust stuck@ y errors, where $y \neq 0$.

Similarly, there have only been few publications on the fault tolerance analysis of QNNs with permanent faults exploiting the inherent features of the application.

Gambardella et al. [19] presented an error injection framework which provides a methodology to assess the error tolerance of QNNs under a single channel stuck@ fault in hardware. They evaluated the error tolerance of CNNs which were trained using SAT and showed that convolutional layers are more sensitive to errors and causes a significant drop in accuracy as compared to fully connected (FC) layers. As concluded from Gambardella et al. [19], while giving comparable accuracy to floating point CNNs, quantized CNNs suffer from high error sensitivity. As they are the preferred choice for deployment, their error tolerance is of particular importance.

Before introducing the FAT methodology, we will provide a motivating example on why fault tolerance of QNNs needs to be addressed for their deployment on embedded devices. The example is reproduced from Gambardella et al. [19] and shows the behaviour of SAT under a particular error model and highlights the deficiency of SAT which we will address using FAT.

A. Motivation

We trained the same QNNs on CIFAR10 i.e. CNVW1A1, CNVW1A2 and CNVW2A2 in SAT using the Brevitas library [35] in PyTorch [36]. The CNNs were evaluated using the error injection framework, using the channel stuck@ error model in which every channel in every layer is stuck at a time. The qualitative metric is the accuracy on the test set, which is computed in presence of the injected error. The pseudo code for the channel stuck@ experiment is given in Algorithm 1, for more details please refer to the work by Gambardella et al. [19].

Algorithm 1: Error injection evaluation (channel stuck@)

```

for every error value: do
  for every layer: do
    for every channel: do
      stuck the channel @ error value and
      calculate accuracy on test set;
    end
    list min and max accuracy observed for the
    layer;
  end
end

```

Table I shows the results for the error injection on CNVW1A1. The network achieved higher accuracy than Gambardella et al. [19] but a very high accuracy drop (down to 50.83% for the worst case in layer 1) can be observed for SAT under single channel stuck@. A drop of $>30\%$ in accuracy might not be acceptable for mission critical applications where lives or reputation of business/organization can be at stake. This significant drop in accuracy under channel stuck@ faults indicates a possible deficiency of SAT to incorporate fault tolerance in the QNNs.

For a more visual representation, in Figure 3 we plot the data from Table I as a scatter plot. In Figure 3 the point

TABLE I: SAT on CNVW1A1 with CIFAR10

Error-free: 84.57%		s@0 accuracy [%]		s@1 accuracy [%]	
Layer	Channels	min	max	min	max
0	64	79.69	84.38	80.94	84.66
1	64	79.81	84.78	50.83	84.45
2	128	76.33	84.67	78.46	84.66
3	128	83.21	84.54	78.17	84.56
4	256	82.63	84.62	82.76	84.71
5	256	84.24	84.75	84.25	84.67
6	512	84.40	84.66	84.38	84.69
7	512	84.50	84.64	84.51	84.63

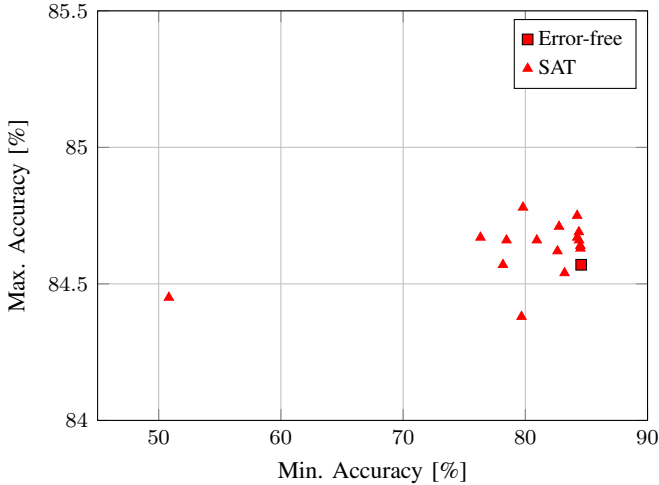


Fig. 3: Error-free and min./max. accuracy under single channel stuck@ error for CNVW1A1 trained with SAT on CIFAR10

representing the minimum accuracy is the leftmost point. The closer the minimum accuracy point is to the error-free point, the higher error tolerance the network exhibits.

In order to guarantee a high minimum accuracy under stuck@ errors, when implementing QNNs trained with SAT, one could apply generic techniques to make CNN inference more reliable. For example, hardware could be deployed with built-in redundancy, such as triple modular redundancy (TMR) [37]. However, as the name suggests, this requires triplicating the DNN hardware and further introduces an overhead in the voting system which is used to make the decision. As such, standard TMR introduces over a 200% increase in compute and memory resources.

In this work we attempt to achieve reliable implementation of QNN hardware accelerators, by exploiting inherent QNN properties to decrease the overall hardware cost. We utilize the inherent redundancy of QNN themselves to make them more tolerant to errors. Specifically, we incorporate stuck@ errors during QNN training which produces highly error tolerant networks, without significantly affecting accuracy or introducing an increase in hardware cost. This work relies on the error injection framework presented by Gambardella et al. [19] which enables fast characterization of the different training methodologies used in this work by means of FPGA acceleration of QNNs.

IV. FAULT AWARE TRAINING

Figure 3 shows high variation among accuracies under single channel stuck@ error model. The goal of FAT is to train QNNs such that they exhibit higher accuracy in presence of errors, thus decreasing the effects of faults within layer and among layers. The main idea is to inject errors (with a certain probability), which matches the error model of our inference hardware during training time. In order to implement the injection at training time, we developed an *error injection layer* which is able to inject stuck@ errors in: channel(s), different pixels in different channels, and same pixel of all channels, depending on the chosen error model.

A. Error Injection Layer

The error injection layer was developed in PyTorch [36] and it allows injecting errors with a particular error model during training. The error injection layer receives a tensor as input in forward pass and injects the errors with a probability p , which is a hyper-parameter. As we chose to inject errors in the activation tensor to match our error model, p represents the global probability of all possible errors to be injected (which depends on the activation precision). Thus each error value has a probability to be injected which is the division of p over the number of possible errors. In the simplest case, the injection layer works as follows: Given an N -dimensional input tensor, $\alpha \in \mathbb{R}^{n_0 \times \dots \times n_{N-1}}$, a random tensor, $\mathbf{r} \in \mathbb{R}^{n_0 \times \dots \times n_{N-1}}$, the output, $\hat{\alpha} \in \mathbb{R}^{n_0 \times \dots \times n_{N-1}}$, of the injection layer is defined as follows:

$$\hat{\alpha}_{\mathbf{i}} = \begin{cases} \epsilon_0 & \text{for } r_{\mathbf{i}} < p_0 \\ \epsilon_1 & \text{for } p_0 \leq r_{\mathbf{i}} < p_1 \\ \vdots & \\ \epsilon_{M-1} & \text{for } p_{M-2} \leq r_{\mathbf{i}} < p_{M-1} \\ \alpha_{\mathbf{i}}, & \text{for } r_{\mathbf{i}} \geq p_{M-1} \end{cases}, \quad (1)$$

where $\mathbf{i} = (i_0, \dots, i_{N-1})$ is a multi-index extracting a single element of an N -dimensional tensor, with $i_n \in \mathbb{Z}^+ \forall n$, $\alpha_{\mathbf{i}}$ is the \mathbf{i}^{th} element of α , $\hat{\alpha}_{\mathbf{i}}$ is the \mathbf{i}^{th} element of $\hat{\alpha}$, $r_{\mathbf{i}} \sim U(0, 1)$ is the \mathbf{i}^{th} element of \mathbf{r} , ϵ_m is the m^{th} possible error value out of total M activation values, where $M = 2^b$, and b is the bitwidth of the activation quantization scheme and finally, p_j is given by:

$$p_j = \frac{p}{100} \frac{j}{M-1}, \quad (2)$$

where $j \in \mathbb{N}_0 \leq M-1$.

Similarly, given the loss gradients, $\frac{\partial L}{\partial \alpha} \in \mathbb{R}^{n_0 \times \dots \times n_{N-1}}$, the input gradients, $\frac{\partial L}{\partial \hat{\alpha}} \in \mathbb{R}^{n_0 \times \dots \times n_{N-1}}$, the backward pass of the injection layer is defined as follows:

$$\frac{\partial L}{\partial \hat{\alpha}_{\mathbf{i}}} = \begin{cases} 0, & \text{for } r_{\mathbf{i}} < p \\ \frac{\partial L}{\partial \alpha_{\mathbf{i}}}, & \text{for } r_{\mathbf{i}} \geq p \end{cases}, \quad (3)$$

where $\frac{\partial L}{\partial \hat{\alpha}_{\mathbf{i}}}$ is the \mathbf{i}^{th} element of $\frac{\partial L}{\partial \hat{\alpha}}$ and $\frac{\partial L}{\partial \alpha_{\mathbf{i}}}$ is the \mathbf{i}^{th} element of $\frac{\partial L}{\partial \alpha}$. Multiple fault models are accommodated within a single injection layer through the definition of \mathbf{r} and

a *broadcasting* function¹, \mathcal{B}_α . For example, the broadcasting function $\mathcal{B}_\alpha(\cdot)$ expands an input tensor by replicating values across every singleton dimension of the input tensor so that it has the same shape as α . For image processing, where the input is a 4D tensor, $\alpha \in \mathbb{R}^{b \times c \times h \times w}$, where $b/c/h/w$ refers to batch size / channels / height / width respectively. In order to inject channel stuck@ errors, \mathbf{r} is defined as:

$$\mathbf{r} = \mathcal{B}_\alpha(\mathbf{r}_c) , \quad (4)$$

where $\mathbf{r}_c \in \mathbb{R}^{b \times c \times 1 \times 1}$, with each element of \mathbf{r}_c is drawn from $U(0, 1)$. The broadcasting function replicates the values of \mathbf{r}_c in the singleton dimensions (height and width, in this example), resulting in identical values within each channel within each batch. When this value of \mathbf{r} is used in Equation (1), the result that each channel is either stuck at a particular value or not. Similarly, for the pixel stuck@ model we have:

$$\mathbf{r} = \mathcal{B}_\alpha(\mathbf{r}_p) , \quad (5)$$

where $\mathbf{r}_p \in \mathbb{R}^{b \times 1 \times h \times w}$, with each element of \mathbf{r}_p is drawn from $U(0, 1)$.

The probability p_i for each of the error value is calculated according to the Equation (2). For example, given a 5% probability p of injection in CNVW1A1, each of the possible error values $\{-1, 1\}$ has a probability of 2.5%. Figure 4 shows an example of forward and backward pass for an FC layer with $A=2$ and possible error values are $\{-1, 0, 1\}$. Whenever the status variable is set to *enable*, the layer is actively injecting errors. On the other hand, setting the status to *disable* will make the injection layer transparent (passing the tensor without injecting errors). The error injection probability in Figure 4 is set at $p=50\%$, hence every activation value in the tensor (abbreviated as α and $\tilde{\alpha}$) has 50% probability of being replaced by error. During backward pass, gradients of the loss with respect to the activations (abbreviated as $\frac{\partial L}{\partial \alpha}$) at the indices at which error was injected, are replaced with zero. This is performed because a small change in the corresponding input activations (which were erroneous after the injection) did not effect the loss value.

Figure 5 shows the insertion of the injection layer in the CNN which is usually composed of repeating blocks i.e. convolution/FC, batch-norm, activation, and sometimes includes pooling. As the injection layer is designed to inject errors in activation tensor, it should be included after activation layer or a pooling layer.

B. Error Injection vs Dropout

The behaviour of the injection layer is conceptually similar to Dropout [38] and Dropout2D [21]. In this subsection, we describe the similarities and differences between our proposed error injection layer and dropout variants. Specifically in this work, we refer to the dropout implementations in PyTorch [36].

Dropout was first introduced by Hinton et al. [38] as a method of reducing overfitting (i.e., improving model generalisation) by preventing the co-adaption of activations. The

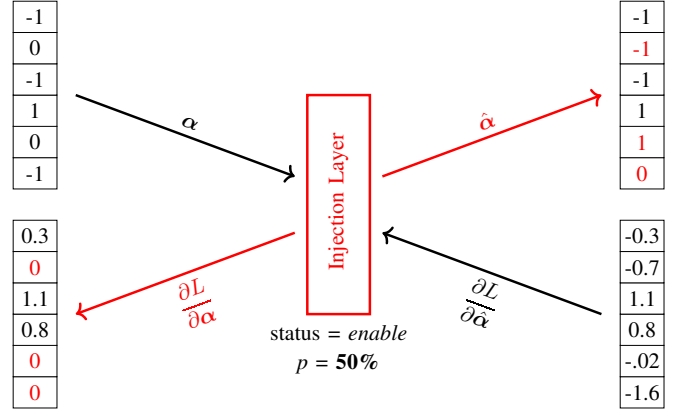


Fig. 4: Forward and backward pass of injection layer

Dropout layer takes an N -dimensional tensor as an input, $\alpha \in \mathbb{R}^{n_0 \times \dots \times n_{N-1}}$, and produces a output tensor, $\tilde{\alpha} \in \mathbb{R}^{n_0 \times \dots \times n_{N-1}}$, with the same shape to the input, but with some values replaced with 0. I.e., some values of α are “dropped out”. To normalise the vector, the remaining values are scaled by $1/(1-p)$, where p is the probability of the neuron being set to zero. Explicitly, the forward path result, $\tilde{\alpha}$, of Dropout is calculated from α and a random tensor $\mathbf{r} \in \mathbb{R}^{n_0 \times \dots \times n_{N-1}}$ as follows:

$$\tilde{\alpha}_i = \begin{cases} 0, & \text{for } r_i < p \\ \frac{1}{1-p} \alpha_i, & \text{for } r_i \geq p \end{cases} , \quad (6)$$

where $\mathbf{i} = (i_0, \dots, i_{N-1})$ is a multi-index, with $i_n \in \mathbb{Z}^+ \forall n$, α_i is the \mathbf{i}^{th} element of α , $\tilde{\alpha}_i$ is the \mathbf{i}^{th} element of $\tilde{\alpha}$ and $r_i \sim U(0, 1)$ is the \mathbf{i}^{th} element of \mathbf{r} . In a standard case, $N = 2$ where n_0 is the batch size and n_1 is the number of neurons in the layer preceding the Dropout layer. Similarly in the backward path, given loss gradients, $\frac{\partial L}{\partial \tilde{\alpha}} \in \mathbb{R}^{n_0 \times \dots \times n_{N-1}}$, the input gradients, $\frac{\partial L}{\partial \alpha} \in \mathbb{R}^{n_0 \times \dots \times n_{N-1}}$, are calculated as follows:

$$\frac{\partial L}{\partial \alpha_i} = \begin{cases} 0, & \text{for } r_i < p \\ \frac{1}{1-p} \frac{\partial L}{\partial \tilde{\alpha}_i}, & \text{for } r_i \geq p \end{cases} , \quad (7)$$

where $\frac{\partial L}{\partial \alpha_i}$ is the \mathbf{i}^{th} element of $\frac{\partial L}{\partial \alpha}$ and $\frac{\partial L}{\partial \tilde{\alpha}_i}$ is the \mathbf{i}^{th} element of $\frac{\partial L}{\partial \tilde{\alpha}}$.

An extension to Dropout, Dropout2D, was introduced by Tompson et al. [21] to extend Dropout to improve its effectiveness in 2D convolutional layers of neural networks. Dropout2d operates on 4-dimensional tensors, with the dimensions, $[n_0, n_1, n_2, n_3]$, usually corresponding to batch size, channels, height and width respectively. Instead of dropping out individual values in the input tensor, Dropout2D drops out and entire channel to zero if the value of $r_i < p$.

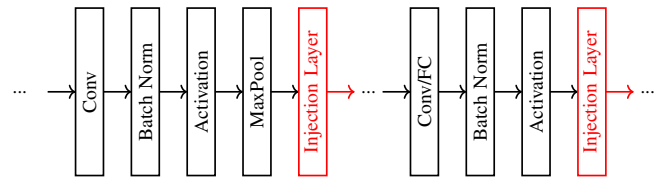


Fig. 5: Injection layer in CNV example

¹<https://numpy.org/doc/stable/user/theory.broadcasting.html>

The injection layer varies from dropout in the following ways:

- it supports injecting all possible fault values into the activations, while dropout only inserts zeros;
- dropout applies scaling to both the outputs and the loss gradients on uncorrupted values, while the error injection layer does not; and
- the error injection layer supports better slicing of the incoming tensor, including stuck@ pixel modes while the dropout variants do not.

C. FAT methodology

After the injection layer is ready to be included in the training of the QNNs, we performed experiments with different configuration of injection layer, error models, and precisions. The probability p of injecting errors is an additional training hyper-parameter which can be set to a fixed value before starting the training process or it can be modified during the training. The value of p needs to be tuned and depends according to the data set, CNN topology and precision. We applied the FAT methodology using the injection layer described in Section IV-A with multiple p values and configurations of the injection layer. In order to characterize the methodology, the first set-up explored (method 1) was training CNNs with:

- Enabling all the injection layers;
- Fixed probability p of injection throughout training.

The second approach (method 2) is based on enabling only one of the injection layers in each training epoch (see Algorithm 2).

Algorithm 2: FAT Method 2

```

for every epoch: do
  enable one random injection layer and disable
  others
  for every batch: do
    | forward and backward pass to train model
  end
end

```

V. EXPERIMENTS AND RESULTS

We trained CNVW1A1, CNVW1A2, CNVW1A3, CNVW1A4, and CNVW2A2 with SAT and FAT, targeting channel stuck@ error model on CIFAR10, GTSRB, SVHN as well as ImageNet (using DoReFa-Net by Zhou et al. [9]). For same pixel in all channel stuck@, we experimented with CNVW1A1, CNVW1A2 and CNVW2A2 on CIFAR10 only. For SAT and FAT the training hyper-parameters were kept the same i.e., 1000 epochs, ADAM optimizer with initial learning rate of 0.02 which was halved every 40 epochs, weight decay set to 0, batch-size of 100 and squared hinge loss. Training was performed on NVIDIA P6000 GPU. The error injection evaluation for CNVW1A1, CNVW1A2 and CNVW2A2 was performed on a Xilinx Zynq UltraScale+ MPSOC ZCU104 [39], Whereas for ImageNet it was performed on multiple GPUs.

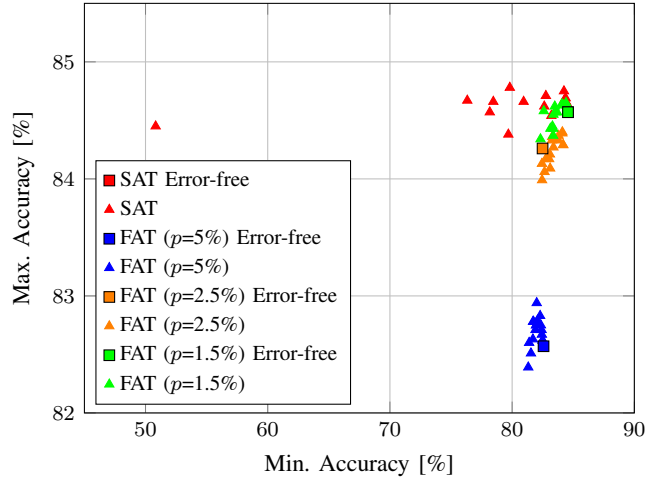


Fig. 6: Error-free and min./max. accuracy under single channel stuck@ error for SAT vs FAT (method 1) on CNVW1A1 with CIFAR10

A. SAT vs FAT Method 1

In method 1 we enabled all injection layers in our CNN with a fixed probability p . Figure 6 shows a comparison between error injection results of SAT CNVW1A1 (same as in Figure 3) and 3 CNVW1A1 trained with FAT (method 1) on CIFAR10 with different probabilities of error injection. For FAT, the injection probabilities are 5%, 2.5% and 1.5% and the error model used is channel stuck@. Note, that the SAT error-free accuracy is occluded by the FAT($p=1%$) error-free accuracy in Figure 6. It can be noticed from the scatter plots that training with FAT makes the CNN more resilient to channel stuck@ errors, given that for all the 3 networks trained with FAT the minimum accuracy in presence of a single channels stuck@ (x -axis in Figure 6) is much closer to the error-free accuracy and it shows a huge improvement. Nonetheless, it can also be noticed how the error-free accuracy in some cases is lower than the SAT one. As expected, by increasing the error injection probability, the CNN increases the robustness against channel stuck@ errors, while decreasing the error-free accuracy. Similarly, by decreasing the value p the error-free accuracy gets closer to the original trained with SAT.

B. SAT vs FAT Method 2

In method 2, only one of the injection layers in the network is kept enabled at a time, with a fixed probability p , while all other injection layers are kept disabled. For this configuration we also trained the networks with different probabilities of error injection i.e. from 1% to 20%. The results for FAT method 2 on CNVW1A1 with 5%, 10% and 15% probability and channel stuck@ error model are given in Figure 7. For method 2 (enabling one layer at a time) it can be observed that both 5% and 10% provides better results than the method 1 (with all the injection layers enabled concurrently). First, in all cases with different p values we always notice a similar improvement as method 1 in presence of single channel stuck@ error i.e. minimum accuracy always being higher than

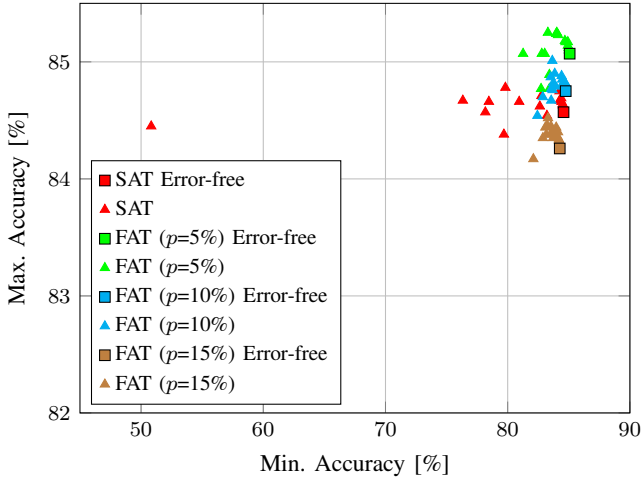


Fig. 7: Error-free and min./max. accuracy under single channel stuck@ error for SAT vs FAT (method 2) on CNVW1A1 with CIFAR10

80%. Second, an improvement in error-free accuracy for low probabilities of error injection i.e. 5% and 10% as compared to SAT can be clearly observed from Figure 7. In Table II, a similar trend was observed for higher precisions. For all of the networks tested, we achieved higher minimum accuracy under single channel stuck@ as well as higher error-free accuracy. Method 2 ($p=5\%$ and 10%) provides better error-free accuracies than method 1 ($p=5\%$) which is 85.07% and 84.75% respectively as compared to 82.57% and the min accuracy is also better for method 2 ($p=10\%$) i.e. 82.43% as compared to 81.32%. Interestingly for higher probabilities of injection e.g. 15%, the error-free accuracy for FAT method 2 was lower than SAT. Finally, it should also be noted that training with FAT comes at no additional convergence time or number of epochs. Since FAT (method 2) outperformed method 1 in most of our experiments, we performed extended experiments on FAT method 2. Furthermore, unless specified otherwise any reference to FAT from this section onwards refers to FAT (method 2). In Table II, we also show results for experiments extended to new datasets, i.e. GTSRB and SVHN (on CNVW1A1), as well as changing the CNN topology i.e. ImageNet (trained using DoReFa-Net by Zhou et al. [9] for which the possible error values in the activations are $\{0, 0.333, 0.666, 1\}$). On all datasets, minimum and error-free accuracies observed with FAT were better than SAT. Figure 8 shows the results on ImageNet with injection probability of 5% and 2.5%. Note, the ‘‘Ref.’’ column in Table II refers to the error-free accuracy of equivalent SAT models from the available literature.

C. Selective Channel Replication with FAT

One of the hardware solutions presented by Gambardella et al. [19] is selective channel replication, in which rather than triplicating a whole CNN (TMR), only selective portion of the network is triplicated. The methodology consist of characterizing all channels of each layer based on their impact on accuracy under channel

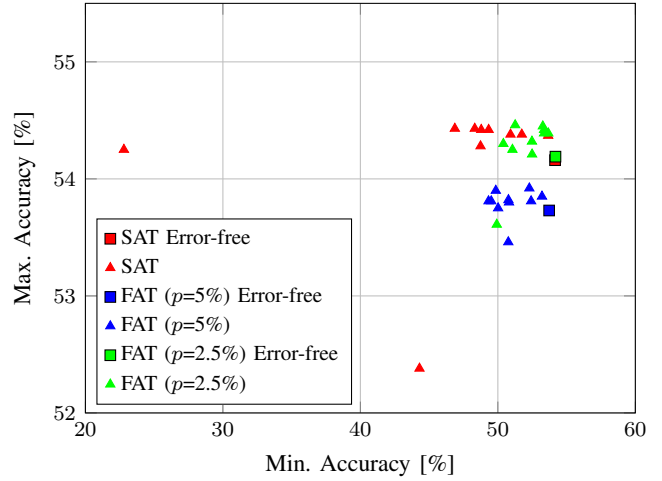


Fig. 8: Error-free and min./max. accuracy under single channel stuck@ error for SAT vs FAT (method 2) on DoReFa-Net with Imagenet

stuck@ error model, sorting them from most to least critical, and triplicating the most critical ones. The amount of channels to triplicate depends on the worst case accuracy in presence of single channel stuck@ that is required to be guaranteed in a system. This provides bigger design space in the hardware cost vs. worst case accuracy trade-off. For example in Figure 9 x -axis is the normalized hardware cost of a fully unrolled model where each MAC operation in the neural network has its own PE, and the y -axis is the worst case error in the presence of single ch stuck@ (in this case, error means the percentage of images that are misclassified, i.e. $100 - \text{minimum accuracy observed}$). On the plot, the right most point of any of the curve represents triplicating all of the channels, hence it costs the maximum hardware but guarantees the same worst case error (under single channel stuck@) as the error free. Whereas the left most point of the curve represents no triplication at all and hence low hardware cost but higher worst case error. Similarly middle points represents triplicating a few channels and the corresponding worst case error. From Figure 9 we can clearly see that FAT offers better trade-offs providing all the pareto dominating solutions in the design space. For example, in order to guarantee 13.84% worst case error for CNVW2A2, SAT requires triplicating 278 channels whereas FAT requires triplicating 2 channels only.

D. FAT vs Dropout2D

In order to compare with FAT, we trained the same networks with Dropout2D. For the Dropout2D experiments, we replicated FAT (method 1), except each error injection layer is replaced with a Dropout2D layer.

Figure 10 shows the results for CNVW1A1 in which an improved minimum accuracy can be observed with both 5% and 2.5% probability of Dropout2D. For example, the minimum accuracy observed under single channel stuck@ is 80.14% as compared to 81.26% of FAT. Table III shows a comparison between Dropout2D and FAT in terms of error-free, minimum

TABLE II: Experiments Summary: SAT vs FAT (channel s@)

Network	Dataset	SAT			FAT				Ref. [%]
		Error-free [%]	Min Acc. [%]	Variance	Error-free [%]	Min Acc. [%]	Variance	Prob. ($p\%$)	
CNVW1A1	CIFAR10	84.57	50.83	1.211	85.07	81.26	0.150	5.0	79.22 [24]
CNVW1A1	CIFAR10	-	-	-	84.75	82.43	0.085	10.0	-
CNVW1A1	CIFAR10	-	-	-	84.25	82.09	0.052	15.0	-
CNVW1A2	CIFAR10	87.46	64.41	2.612	88.31	84.78	0.153	5.0	82.66 [24]
CNVW1A2	CIFAR10	-	-	-	87.72	84.77	0.092	10.0	-
CNVW1A3	CIFAR10	89.21	80.06	2.331	89.73	87.90	0.089	5.0	-
CNVW1A4	CIFAR10	89.13	80.69	1.960	89.74	88.45	0.074	5.0	-
CNVW2A2	CIFAR10	88.25	67.98	2.508	88.96	86.07	0.057	5.0	84.29 [24]
CNVW2A2	CIFAR10	-	-	-	88.60	86.66	0.043	10.0	-
CNVW1A1	SVHN	95.73	94.15	0.04	95.95	95.14	0.01	5.0	94.90 [24]
CNVW1A1	GTSRB	98.11	95.89	0.06	98.70	98.00	0.01	5.0	98.08 [24]
DoReFa-Net	ImageNet	54.16	22.80	2.93	54.19	49.92	0.78	2.5	49.80 [9]

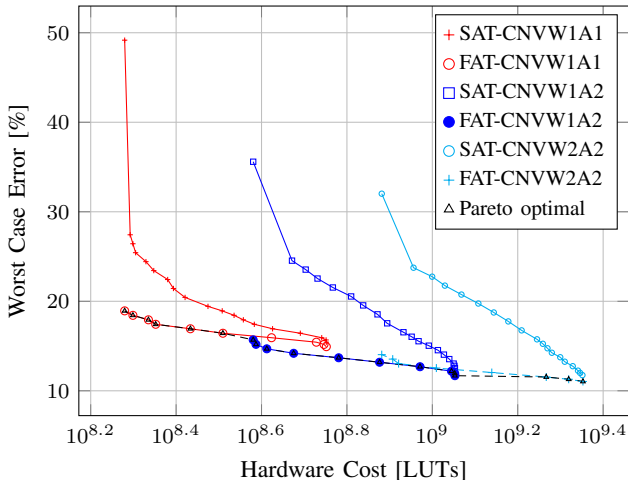


Fig. 9: Pareto frontier of worst-case test error vs. hardware cost with selective channel replication

accuracy and overall variance in the accuracies observed. As shown in the table, Dropout2D also performs very well in terms of error-free accuracy, outperforming FAT in 2 of the 5 networks tested. In terms of minimum accuracy, surprisingly, Dropout2D outperforms FAT in 4 of the 5 networks tested. Although in the average case, there is little difference between the accuracy of FAT and Dropout2D for both error-free and minimum accuracy. There are a few exceptions, notably networks CNVW1A1, CNVW1A3 and CNVW1A4 have approximately a 1% accuracy difference in the minimum accuracy. Both techniques can be considered very effective in improving the minimum accuracy under a single channel stuck@ error model. A surprising observation, is that even though Dropout2D only injects 0-values into tensors it appears robust to stuck@ errors associated with larger integer values, such as 7 and 15, as shown by the results of the cnvW1A3 and cnvW1A4 networks. This will be investigated in further future works.

As Dropout2D achieves similar results to FAT for the channel stuck@ error model in the experiments performed on QNNs, we performed additional experiments on different error model. Table IV shows a detailed comparison among SAT, FAT and Dropout2D on the same pixel stuck@ error

model (shown in the right side of Figure 2). The networks were evaluated with same pixel stuck@ injection, in which we iterate over all pixels in the (*height*, *width*) dimension of the tensor and stuck that pixel for all channels to a particular error value. For FAT and Dropout2D, we experimented with different probabilities and the best results achieved in term of minimum accuracies are listed in Table IV. Similar to the single channel stuck@ model, the QNNs trained with SAT exhibit a high drop in accuracy in presence of single pixel stuck@ error. For example, CNVW1A2 suffers from a drop of >20% accuracy, from 87.46% in the error-free case down to 64.93%. The networks trained with FAT method 2 while injecting errors according to the pixel stuck@ error model shows higher error-free accuracy, as well as very high tolerance to single pixel stuck@ errors as compared to SAT. CNVW1A1, CNVW1A2, and CNVW2A2 trained with FAT shows a drop of 1.43%, 1.51%, and 1.13% respectively, showing a similar trend to the experiments for channel stuck@ listed in Table III. As compared to SAT, Dropout2D shows increase in accuracy as well, in the presence of single error, while in all tested cases FAT outperformed Dropout2D. We believe that the regularization effect provided by Dropout2D is very promising in terms of tolerance for only some error models. Nonetheless, the results in Table IV show that during training, it is important to adopt the error model which better represents possible hardware faults in the target accelerator. FAT provides this additional level of flexibility. It is possible, that with more flexible control over the dropout pattern in the output tensor, Dropout will also perform well for this error model.

VI. OBSERVATIONS, DISCUSSION AND SUGGESTIONS

It can be seen from the results in Section V that the FAT methodology helps in training error tolerant QNNs. The error injection during training also acts as a regularizer and prevents overfitting, thus increasing the accuracy of the model. When using method 1 with the higher probability of error injection i.e. >5% very low variance in accuracies can be achieved but at the expense of lower error-free accuracy. Depending upon the application in which CNNs is going to be deployed, if low variance among accuracies in presence of faults is the primary concern then method 1 is more suitable. Whereas if

TABLE III: Experiments Summary: FAT vs Dropout2D (channel s@)

Network	Dataset	FAT				Dropout2D			
		Error-free [%]	Min Acc. [%]	Variance	Prob. (p%)	Error-free [%]	Min Acc. [%]	Variance	Prob. (p%)
CNVW1A1	CIFAR10	85.07	81.26	0.150	5.0	84.41	80.14	0.132	2.5
CNVW1A2	CIFAR10	88.31	84.78	0.153	5.0	88.36	85.07	0.113	2.5
CNVW1A3	CIFAR10	89.56	87.27	0.089	2.5	89.50	88.38	0.073	2.5
CNVW1A4	CIFAR10	89.41	87.86	0.074	2.5	89.36	88.60	0.079	2.5
CNVW2A2	CIFAR10	88.96	86.07	0.057	5.0	89.47	86.33	0.089	2.5

TABLE IV: Experiments Summary: SAT vs FAT vs Dropout2D (same pixel s@)

Network	Dataset	SAT		FAT		Dropout2d			
		Error-free [%]	Min Acc. [%]	Prob. (p%)	Error-free [%]	Min Acc. [%]	Prob. (p%)	Error-free [%]	Min Acc. [%]
CNVW1A1	CIFAR10	84.57	79.83	2.5	85.03	83.60	2.5	84.41	81.14
CNVW1A2	CIFAR10	87.46	64.93	2.5	88.06	86.55	10.0	88.50	82.48
CNVW2A2	CIFAR10	88.25	71.34	2.5	89.13	88.00	10.0	87.70	83.71

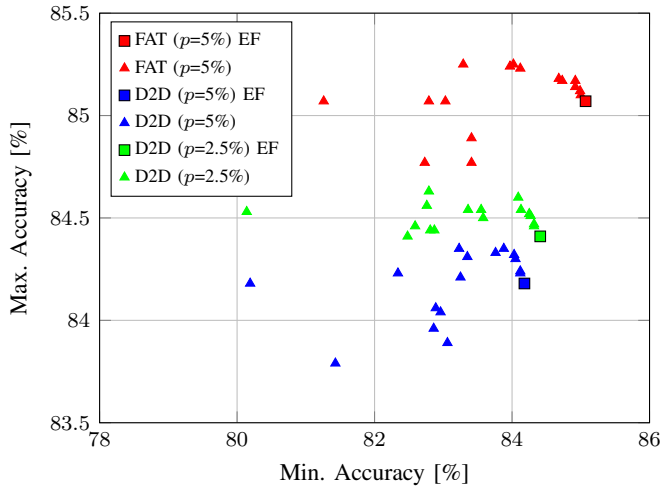


Fig. 10: FAT vs Dropout2D (D2D) on CNVW1A1 with CIFAR10 of both error-free (EF) and with a single channel stuck@ error

the high error-free accuracy is of higher priority then method 2 is recommended.

In our experiments, we found that values of p in the range of 1-10% resulting in the best error-free and worst-case accuracy. Enabling one injection layer per epoch (method 2) and training from scratch is recommended to get a better minimum accuracy and lower overall variance in worst-case accuracy.

VII. CONCLUSION

In this work we presented a new method for training an efficient error tolerant QNNs called FAT. We showed that training with FAT yields highly accurate and error tolerant QNNs at no additional accuracy and convergence cost. To the best of our knowledge FAT outperforms all existing work targeting stuck@0 faults. In addition, we showed that training QNNs with FAT can also improve the error-free accuracy, suggesting that FAT may behave like a regularizer, to improve generalization of QNNs to the test set. We also showed that a variant of Dropout, Dropout2D, can be used to significantly improve the tolerance of QNNs to stuck@ faults, which provides similar performance to FAT to for single channel stuck@

errors. However, we also showed the importance of injecting errors during training which matches the associated fault model, in particular, showing that FAT outperforms Dropout2D in the same pixel stuck@ case. We also showed that FAT offers an improved hardware cost vs. worst case error trade off when compensating for errors in hardware. We are planning to extend our investigation and explore FAT for different error models, higher precision, alternative layer types and alternative architectures. Furthermore, in this work we applied FAT to popular benchmarks, in future works we plan to apply these techniques to applications with strict accuracy requirements under hardware faults and to more complex training regimes, such as reinforcement learning and generative adversarial networks. Lastly, we also plan to investigate ways to further scale the error injection evaluation campaign, in order to allow more complex network topologies to be explored.

REFERENCES

- [1] A. Krizhevsky, I. Sutskever, and G. E. Hinton, “Imagenet classification with deep convolutional neural networks,” ser. NIPS’12, 2012, pp. 1097–1105.
- [2] J. Redmon, S. Divvala, R. Girshick, and A. Farhadi, “You only look once: Unified, real-time object detection,” in *2016 IEEE CVPR*, 2016, pp. 779–788.
- [3] V. Badrinarayanan, A. Kendall, and R. Cipolla, “SegNet: A deep convolutional encoder-decoder architecture for image segmentation,” *IEEE TPAMI*, vol. 39, no. 12, pp. 2481–2495, 2017.
- [4] O. Ronneberger, P. Fischer, and T. Brox, “U-Net: Convolutional networks for biomedical image segmentation,” in *MICCAI 2015*, pp. 234–241.
- [5] K. He, X. Zhang, S. Ren, and J. Sun, “Delving deep into rectifiers: Surpassing human-level performance on imagenet classification,” in *ICCV*, 2015, pp. 1026–1034.
- [6] P. Gysel, J. Pimentel, M. Motamedi, and S. Ghiasi, “Ristretto: A framework for empirical study of resource-efficient inference in convolutional neural networks,” *IEEE TNNLS*, 2018.
- [7] M. Courbariaux, I. Hubara, D. Soudry, R. El-Yaniv, and Y. Bengio, “Binarized neural networks: Training deep

- neural networks with weights and activations constrained to +1 or -1,” *arXiv preprint arXiv:1602.02830*, 2016.
- [8] M. Rastegari, V. Ordonez, J. Redmon, and A. Farhadi, “XNOR-Net: Imagenet classification using binary convolutional neural networks,” in *ECCV 2016*.
- [9] S. Zhou, Y. Wu, Z. Ni, X. Zhou, H. Wen, and Y. Zou, “DoReFa-Net: Training low bitwidth convolutional neural networks with low bitwidth gradients,” *arXiv preprint arXiv:1606.06160*, 2016.
- [10] Z. Cai, X. He, J. Sun, and N. Vasconcelos, “Deep learning with low precision by half-wave gaussian quantization,” pp. 5918–5926, 2017.
- [11] S. Han, H. Mao, and W. J. Dally, “Deep compression: Compressing deep neural networks with pruning, trained quantization and huffman coding,” *arXiv preprint arXiv:1510.00149*, 2015.
- [12] A. G. Howard, M. Zhu, B. Chen, D. Kalenichenko, W. Wang, T. Weyand, M. Andreetto, and H. Adam, “Mobilenets: Efficient convolutional neural networks for mobile vision applications,” vol. abs/1704.04861, 2017.
- [13] B. Wu, A. Wan, X. Yue, P. H. Jin, S. Zhao, N. Golmant, A. Gholaminejad, J. Gonzalez, and K. Keutzer, “Shift: A zero flop, zero parameter alternative to spatial convolutions,” *CoRR*, vol. abs/1711.08141, 2017.
- [14] N. J. Fraser, Y. Umuroglu, G. Gambardella, M. Blott, P. Leong, M. Jahre, and K. Vissers, “Scaling binarized neural networks on reconfigurable logic,” ser. PARMA-DITAM '17. New York, NY, USA: Association for Computing Machinery, 2017, p. 25–30.
- [15] S. Tripathi, G. Dane, B. Kang, V. Bhaskaran, and T. Q. Nguyen, “Lcdet: Low-complexity fully-convolutional neural networks for object detection in embedded systems,” *CoRR*, vol. abs/1705.05922, 2017.
- [16] Y. Umuroglu, N. J. Fraser, G. Gambardella, M. Blott, P. Leong, M. Jahre, and K. Vissers, “Finn: A framework for fast, scalable binarized neural network inference,” in *FPGA-17*. ACM, pp. 65–74.
- [17] S. Carlier, M. Coindoz, L. Deneuville, L. Garbellini, and A. Altavilla, “Evaluation of reliability, availability, maintainability and safety requirements for manned space vehicles with extended on-orbit stay time,” *Acta Astronautica*, vol. 38, no. 2, pp. 115 – 123, 1996.
- [18] W. Goble and A. Brombacher, “Using a failure modes, effects and diagnostic analysis (fmeda) to measure diagnostic coverage in programmable electronic systems,” *Reliability Engineering & System Safety*, pp. 145 – 148, 1999.
- [19] G. Gambardella, J. Kappauf, M. Blott, C. Doehring, M. Kumm, P. Zipf, and K. Vissers, “Efficient error-tolerant quantized neural network accelerators,” in *DFT 19*, Oct. 2019.
- [20] N. Khoshavi, C. Broyles, and Y. Bi, “A survey on impact of transient faults on bnn inference accelerators,” *arXiv preprint arXiv:2004.05915*, 2020.
- [21] J. Tompson, R. Goroshin, A. Jain, Y. LeCun, and C. Brengle, “Efficient object localization using convolutional networks,” in *CVPR*, 2015.
- [22] S. Mittal, “A survey of fpga-based accelerators for convolutional neural networks,” *Neural Computing and Applications*, Oct 2018.
- [23] S. I. Venieris, A. Kouris, and C.-S. Bouganis, “Toolflows for Mapping Convolutional Neural Networks on FPGAs: A Survey and Future Directions,” *ACM Computing Surveys (CSUR)*, vol. 51, no. 3, pp. 56–39, Jul. 2018.
- [24] M. Blott, T. Preusser, N. Fraser, G. Gambardella, K. O’Brien, and Y. Umuroglu, “FINN-R: An end-to-end deep-learning framework for fast exploration of quantized neural networks,” *ACM TRETS*, 2018.
- [25] [Online]. Available: <https://github.com/Xilinx/BNN-PYNQ/>
- [26] S. Jha, T. Tsai, S. Hari, M. Sullivan, Z. Kalbarczyk, S. W. Keckler, and R. K. Iyer, “Kayotee: A fault injection-based system to assess the safety and reliability of autonomous vehicles to faults and errors,” *arXiv preprint arXiv:1907.01024*, 2019.
- [27] G. Li, S. K. S. Hari, M. Sullivan, T. Tsai, K. Pattabiraman, J. Emer, and S. W. Keckler, “Understanding error propagation in deep learning neural network (dnn) accelerators and applications,” in *SC '17*, 2017, pp. 8:1–8:12.
- [28] K. Pei, Y. Cao, J. Yang, and S. Jana, “Deepxplore: Automated whitebox testing of deep learning systems,” *Commun. ACM*, vol. 62, no. 11, p. 137–145, Oct. 2019.
- [29] D. Deodhare, M. Vidyasagar, and S. Sathiy Keethi, “Synthesis of fault-tolerant feedforward neural networks using minimax optimization,” *IEEE TNN*, vol. 9, no. 5, pp. 891–900, Sep. 1998.
- [30] P. Dey, K. Nag, T. Pal, and N. R. Pal, “Regularizing multilayer perceptron for robustness,” *IEEE SMC*, vol. 48, no. 8, pp. 1255–1266, Aug 2018.
- [31] Y. Tan and T. Nanya, “Fault-tolerant back-propagation model and its generalization ability,” in *IJCNN-9*, vol. 3, Oct 1993.
- [32] C. H. Sequin and R. D. Clay, “Fault tolerance in artificial neural networks,” in *IJCNN*, June 1990, pp. 703–708.
- [33] C. Neti, M. H. Schneider, and E. D. Young, “Maximally fault tolerant neural networks,” *IEEE Trans. Neural Netw.*, vol. 3, no. 1, pp. 14–23, Jan 1992.
- [34] V. Duddu, D. V. Rao, and V. E. Balas, “Adversarial fault tolerant training for deep neural networks,” *arXiv preprint arXiv:1907.03103*, 2019.
- [35] [Online]. Available: <https://github.com/Xilinx/brevitas/>
- [36] A. Paszke, S. Gross, F. Massa, A. Lerer, J. Bradbury, G. Chanan, T. Killeen, Z. Lin, N. Gimelshein, L. Antiga, A. Desmaison, A. Kopf, E. Yang, Z. DeVito, M. Raison, A. Tejani, S. Chilamkurthy, B. Steiner, L. Fang, J. Bai, and S. Chintala, “Pytorch: An imperative style, high-performance deep learning library,” in *NIPS 32*, 2019, pp. 8024–8035.
- [37] R. E. Lyons and W. Vanderkulk, “The use of triple-modular redundancy to improve computer reliability,” *IBM Journal of Research and Development*, 1962.

- [38] G. E. Hinton, N. Srivastava, A. Krizhevsky, I. Sutskever, and R. R. Salakhutdinov, "Improving neural networks by preventing co-adaptation of feature detectors," *arXiv preprint arXiv:1207.0580*, 2012.
- [39] [Online]. Available:
<https://www.xilinx.com/products/boards-and-kits/zcu104.html>